Al-Rafidain Engineering Journal (AREJ) Vol. 30, No. 2, September 2025, pp. 116-123

Performance Evaluation of Combined Cycle Gas Turbine Integrated with Concentrated Solar Power System

Rahmah Luqman Ibrahim
rahma.21enp85@student.uomosul.edu.iq

Abdulrahaman Habbo Mohammed
abidhabbo20@uomosul.edu.iq

Mechanical Engineering Department, College of Engineering, University of Mosul, Mosul, Iraq

Received: March 6th, 2025, Received in revised form: July 10th, 2025, Accepted: August 3rd, 2025

ABSTRACT

The development of simple gas power plants is attracting significant interest. In this regard, the possibility of developing a simple gas power plant with a capacity of (125MW) is being discussed. The first stage represents the utilizing of the thermal energy carried by the exhaust gases coming out of the simple gas turbine unit, by combining the gas turbine unit with a steam turbine unit through a dual-heat recovery steam generator, to form the combined cycle gas turbine unit. As for the second stage, it is represented by capitalizing on the solar energy through integrating the latter with the solar energy field, to form the integrated solar combined cycle unit. The results show that the advantages obtained from the first stage are high power output, thermal efficiency and, best specific fuel consumption, which can be obtained at (185.423MW), (49.77%) and (0.147kg/kW.hr) respectively. Regarding the second phase, the results show that adding a solar collector contributed to increasing the amount of steam entering the steam unit. As a result, the power output and thermal efficiency of the combined cycle unit increased to (207.964MW) and (55.3%), respectively. As for the specific fuel consumption, it reached (0.1315kg/kW.hr).

Keywords:

Combined cycles gas turbines; dual-heat recovery steam generator; integrated solar combined cycle unit; solar collector.

https:// https://rengj.uomosul.edu.iq
Email: alrafidain_engjournal3@uomosul.edu.iq

===

1. INTRODUCTION

Most of the gas units operating in Iraq are of the simple cycle type, whose disadvantages are low generating capacity and poor thermal efficiency of no more than 35%. This is because 65% of the thermal energy is wasted to the surrounding environment with the exhaust gases. In recent days, most of the countries that depend on simple gas units for their energy tend to develop and convert them into combined generating units by combining a gas unit with a steam unit using a Heat Recovery Steam Generator (HRSG), Figure (1 -A). This study focuses on the possibility of using solar energy collectors and integrating them with the combined generating units of the Al-Amara gas station to configure Integrated Solar Combined Cycle (ISCC). The idea of ISCC dates back to the early nineties, when it was proposed by a company (Luz Solar International). In 2015, these stations began to spread in many countries [1]. After that, many researchers in this field studied these units in terms of performance, economics and design point of view. The two researchers (Bashir & Özbey) conducted a theoretical study to design a concentrated solar power station of the parabolic basin type in Sudan. To analyze the economic and technical feasibility, the researchers used the System Advisor Model (SAM) program to determine the best site for establishing the solar station in 15 cities in Sudan. Its purpose is to obtain the highest radiation intensity and the lowest wind speed, considering the provision of water resources, as well as the vast unexploited areas and access to the electrical network [2]. The researchers (Alqahtani & Patiño-Echeverri) conducted a theoretical study in which the advantages of the integrated combined generation unit with solar energy were determined in terms of economic and environmental aspects, using the Concentrated Solar Power (CSP) technology with the use of an energy storage system [1]. The researcher (Li) and his colleagues conducted a theoretical study of the ISSC unit. The study incorporated a comparison between two systems: one using thermal storage and another without thermal storage. The researchers also addressed the economic aspect. They concluded that the highest achievable efficiency is obtained when there is no thermal storage. As for the economic aspect, which included operating, maintenance, and fuel costs, the cost for the thermal storage system was higher at 1.388$ per kilowatt-hour compared to the system without storage. [3]. (Peterseim) and others studied the possibility of integrating a combined generating unit with a concentrated solar energy technology of the type of solar energy tower with the use of a thermal storage system for molten salt sufficient to generate electrical energy for a period of three hours. The researchers described the ideal sites for using the combined generation unit integrated with solar energy in western Australia. The results show that the use of the solar power tower system has contributed to increasing the efficiency of the combined generating unit. The researchers also concluded that converting a conventional combined cycle unit into an ISCC unit is promising in terms of the payback period of the construction cost [4]. ISCC is operated either as a Direct Steam Generator (DSG) or by using a separate liquid such as thermal oil. In this paper, the ISCC-DSG technology, shown in Figure (1 - B), will be used. This technology is considered the best option, especially in arid countries rich in natural gas, such as Iraq [5]. Some of the ISCC power plants in the world which depended on the technology of DSG for twenty years are found in Kuwait, Algeria, China, and India. [6]. The proposed design of ISCC is flexible in the operating system. During nighttime, it works as a conventional Combined Cycle Gas Turbine (CCGT) and during daytime, it works as ISCC. Typical ISCC system consists of four main components: Gas Turbine (GT), HRSG, Steam Turbine (ST) and the solar filed. There are four types of CSP technologies: parabolic trough collector, solar power tower, linear Fresnel reflector, and parabolic dish reflector [7]. Parabolic trough technology is Considered as one of the widely used types. It occupies 90% of the total CSP technologies used in solar power plants for decades [8], and it is adopted in the present study. The basic working principle of the ISCC system first involves, operating the combined generating unit by utilizing the exhaust gases from the gas turbine unit, while the solar energy field supports the combined generating unit by producing steam that is added to the steam turbine.

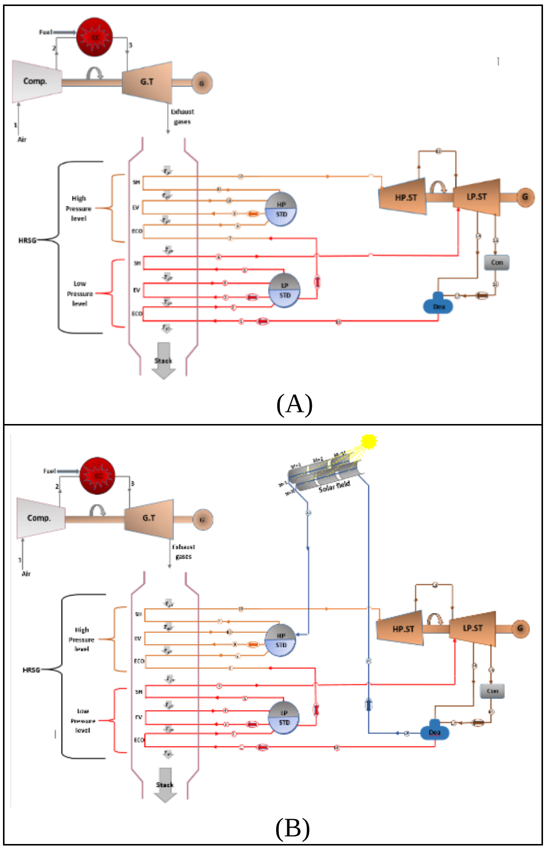

Fig. 1 (A) Combined cycles gas turbines system (B) Integrated solar combined cycle system

2. MATHEMATICAL MODEL

In order to evaluate the performance of the solar collector and its effect on the combined cycle power plant, it is necessary to calculate the direct solar radiation from sunrise to sunset, some of the important angles are shown in Figure (2). Also, a thermodynamic model of ISCC system is given, and the simulation is done by Engineering Equations Solver (EES) software.

2.1. Estimation of the Clear Sky Radiation

For the assessment of the solar radiation transmitted through the clear atmospheres, (The Hottel method) will be used. The selected intensity of solar radiation corresponds to 12:00 noon on the 21^{st} of June. The proposed location is in southern Iraq, in the city of Al-Amara (latitude: 31.84°, longitude: 47.15°). The solar radiation transmitted through the atmosphere is divided into three parts: solar radiation that is not scattered is called beam radiation, the scattered solar radiation is called diffuse radiation, and the total amount of solar radiation, including both beam and diffuse components, is called total solar radiation as shown in Figure (3). The intensity of extraterrestrial radiation outside the atmosphere (G_{on}) is calculated using the following equation [9].

$$G_{on} = G_{sc}\left[1 + 0.033\cos\frac{360\,n}{365}\right] \qquad (1)$$

The clear sky beam (G_{cb}) and diffuse radiation (G_{cd}) are calculated using the following equation [10].

$$G_{cb} = G_{on}\,\tau_b\,\cos\theta_z \qquad (2)$$
$$G_{cd} = G_{on}\,\tau_d\,\cos\theta_z \qquad (3)$$

The atmospheric permeability coefficient for diffuse and beam radiation is calculated using the following equation [11].

$$\tau_d = 0.271 - 0.294\,\tau_b \qquad (4)$$

$$\tau_b = a_o + a_1\,exp\left(-\frac{K_s}{cos\,\theta_z}\right) \qquad (5)$$

Constants a_o^* , a_1^* and K^* are used for the standard atmosphere with 23 km visibility. The unknowns constants a_o , a_1 and K_s are used to calculate the climate of an area which are given for altitudes below 2.5 km can be calculated from the following relationships [12].

$$a_o^* = 0.4237 - 0.00821 \times (6 - \mathrm{Z})^2 \qquad (6)$$
$$a_1^* = 0.5055 + 0.00595 \times (6.5 - \mathrm{Z})^2 \qquad (7)$$
$$K^* = 0.2711 + 0.01858 \times (2.5 - \mathrm{Z})^2 \qquad (8)$$

where (Z) represents the elevation (km) above sea level for the selected study area.

$$a_o = r_o \times a_o^* \qquad a_1 = r_1 \times a_1^* \qquad K_s = r_k \times k^*$$

where r_o , r_1 and r_k are correction factors that can be found in Table (1).

Table 1: Correction Factors for Climate Type [11].

Climate type	Tropical	Mid-latitude summer	Subarctic summer	Mid-latitude winter
r_o	0.95	0.97	0.99	1.03
r_1	0.98	0.99	0.99	1.01
r_k	1.02	1.02	1.01	1.00

The solar angle of incidence (θ) is the angle between the incident solar radiation and the normal to the inclined receiving surface. It can be obtained from the following relationship [13].

$$\cos\theta = (1 - \cos^2\delta\ \sin^2\omega)^{\frac{1}{2}} \qquad (9)$$

The solar declination angle (δ) represents the angle that affects the determination of the seasons of the year, as the values of the declination angle change within the range $(-23.45°$ to $23.45°)$ for the summer and winter solstices, and the spring and autumn equinoxes, respectively. The solar declination angle varies throughout the year for and can be approximately calculated by the following equation for any day (n) [14].

$$\delta = 23.45 \times sin\left[\frac{360}{365} \times (284 + n)\right] \qquad (10)$$

The hour angle (ω) is the angle formed by the Earth's rotation around its axis so that the longitude of a point falls under the sun's rays, where this angle is positive during the pre-noon periods, zero at noon, and negative in the afternoon. It is assumed that the Earth rotates at a rate of 15 degrees per (360°/24 hours). It is expressed as follows [13].

$$\omega = (hour - 12) \times 15 \qquad (11)$$

The Solar zenith angle (θ_z), which is the angle between the incident solar radiation and the normal to the horizontal receiver surface (when tilt angle is equal to zero). it is given by equation [13].

$$\cos\theta_z = \cos\varphi\,.\cos\delta\,.\cos\omega + \sin\varphi\,.\sin\delta \qquad (12)$$

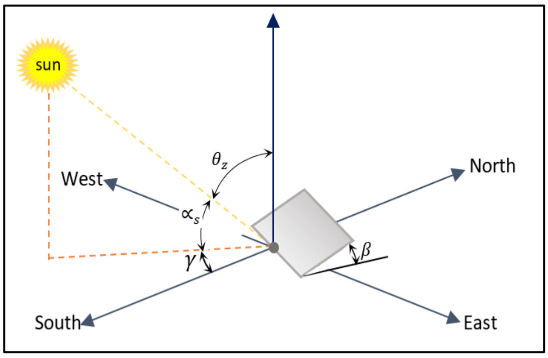

Fig. 2 Some of the solar angles

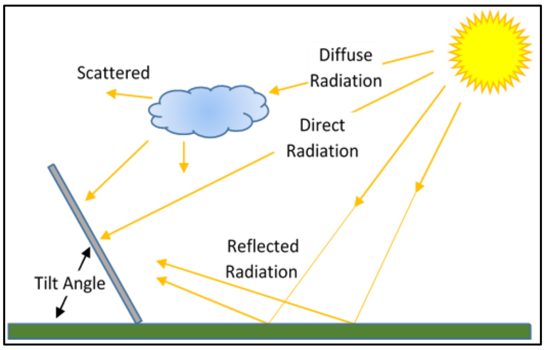

Fig. 3 Beam and diffuse solar radiation

2.2. Solar Filed Analysis

The solar field consists of numerous Parabolic Trough Collectors (PTCs). The useful energy gain depends on the collector 's overall optical efficiency and incident angle modifier, in addition to some factors affect the system performance by loss factors such as end shading, tube soiling, and inter-row shading. It can be calculated by the following equations:

The solar energy absorbed by the heat collector tube can be calculated by equation [14].

$$Q_{abs} = G_{cb}.\mathrm{k}_{\theta}.\eta_{opt}.f_{clean}.\cos\theta .f_{rowshading}.f_{endloss} \quad (13)$$

η_{opt} : The collector overall optical efficiency depends upon collector reflectance, receiver absorbance, glass envelope transmittance and intercept factor [14].

$k_{(\theta)}$: Incident angle modifier for Luz (LS-3) is given in [15].

$f_{rowshading}$: The row shading factor is the performance factor representing mutual shading of parabolic collector rows during early morning periods and late in the evening [16].

$f_{endloss}$: The solar loss factor happens from the ends of the heat collector tube [16].

The useful solar field energy gain per row can be calculated by the relationship [15].

$$Q_{usf} = Q_{abs}(w_a - D_{ro})\, L\, M - Q_{loss} \quad (14)$$

2.3. Integrated Solar Combined Cycle Analysis

The present research develops a mathematical model the of the ISCC power plants. Mass and energy conservation laws were utilized to the GT and ST units, the HRSG and the solar field. To evaluate the performance of the ISCC power plants, the electricity production in the plant is determined as follows:

The power output of the ISCC power plants can be given by [17].

$$Pe_{ISCC} = Pe_{sf} + Pe_{CCGT} \quad (15)$$

The Thermal efficiency of the ISCC power plants is given by equation [18].

$$\eta_{ISCC} = \frac{\mathrm{Pe_{ISCC}}}{\dot{m}_{f}\,\mathrm{LCV} + A_{sf}\,G_{cb}} \quad (16)$$

The specific fuel consumption of the ISCC power plants is calculated by the equation:

$$\mathrm{SFC_{ISCC}} = \frac{\dot{m}_{f} \times 3600}{\mathrm{Pe_{ISCC}}} \quad (17)$$

3. RESULTS AND DISCUSSIONS

A mathematical model of typical ISCC systems is developed in this paper. Mass and energy conservation laws were applied to the gas and steam turbine units, the HRSG and the PTC of solar field using the EES software to evaluate the performance of the ISCC system. Al-Amara has a good sunny period on the 21^{st} of June to obtain the following results.

3.1. The Solar Filed

In order to evaluate the performance of the solar field, it is necessary to estimate the best solar declination angle during the months of the year and the intensity of solar radiation from sunrise to sunset. The value of the solar declination angle, as shown in Figure (4), starts to increase in January and gradually diminishes in December. Their values are negative due to the occurrence of solar radiation perpendicular to the Tropic of Capricorn, where the southern part of the globe (below the equator) is most exposed to the sun's rays. This results in shorter daylight hours and longer nighttime hours. As for the month of June, the solar declination angle is positive and reaches its peak because the solar radiation is focused on the Tropic of Cancer (above the equator). Thus, the northern part is exposed to the sun's rays, resulting in longer daylight hours and shorter night hours. Then, it gradually starts to decrease during the spring and autumn seasons. The night and day periods are almost equal due to the occurrence of solar radiation on the equator.

The three types of solar radiation, direct, diffuse and total, are shown in Figure (5). The least possible amount of solar radiation occurs at sunrise and sunset, because it travels through the longest path in the atmosphere, which happens when the angle of incidence is ($\propto_s$=0°). At midday, solar radiation reaches its peak because the angle of incidence is vertical ($\propto_s$=90°), and the radiation travels the shortest distance through the atmosphere. Therefore, the amount of solar radiation received is at its maximum. Then, its value begins to decrease symmetrically until sunset. in Figure (6), the highest amount of the solar radiation occurs in June, while the lowest occurs in December, in March and September, the angle of solar incidence takes similar values. This is due to the position of the sun relative to the Earth, as shown by the solar declination angle in Figure (4). This figure also shows that the times of sunrise and sunset vary with the seasons due to the effect of the hour angle. Figure (7) shows that the total mass of the fluid is at its lowest at sunrise, increases further to reaches its maximum at midday and, then decreases at sunset. This is due to the variation in the amount of useful energy gained from the solar fields.

The thermal efficiency of the solar field, as shown in Figure (8), increases with the intensity of solar radiation from sunrise; it increases to reach its highest value at midday, and then decreases at sunset. This behavior is attributed to its depends on the amount of useful energy gain and beam solar radiation.

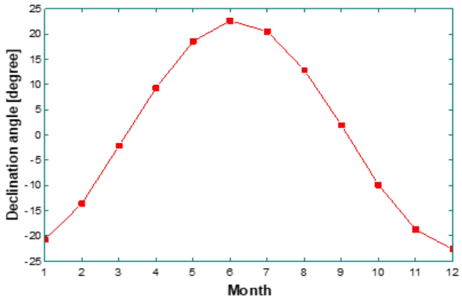

Fig. 4 The declination angle throughout the year.

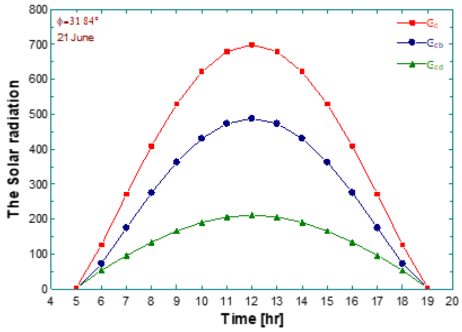

Fig. 5 The solar radiation at selected dates.

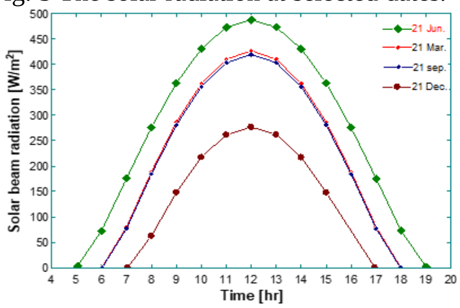

Fig. 6 The solar beam radiation at selected dates.

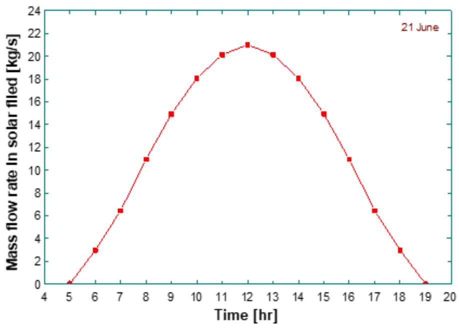

Fig. 7 The mass of the fluid passing through the solar fieldenergy at selected dates.

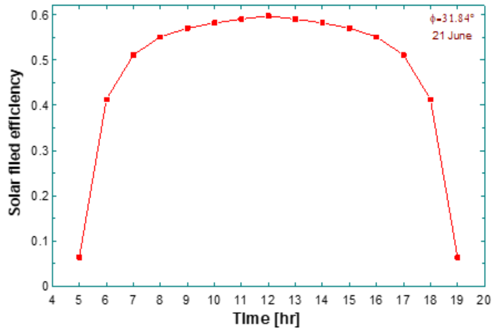

Fig. 8 The efficiency of the solar fieldat selected dates.

3.2. The ISCC System

In order to evaluate the integrated plant, it is necessary to estimate its electricity production and efficiency as well as the specific fuel consumption of the power plant. The capacity of the combined cycle power plant, as shown in Figure (9), increases when integrated with the solar field. This increase varies throughout the day. It rises with increasing solar radiation intensity, reaching its peak at noon; then it begins to decrease until sunset. This can be explained by the increase in the amount of steam generated from the solar field, which is added to the HRSG. It was also noted that the thermal efficiency of the ISCC power plant, illustrated in Figure (10), increases. It reaches its highest value at noon; then, it begins to decrease to reach its lowest value by sunset. This behavior is directly due to the power of the ISCC, which affects thermal efficiency. The specific fuel consumption of ISCC, as presented in Figure (11), decreases, reaching its lowest value at noon. Then, it begins to increase by sunset due to its effect on the integrated combined generation capacity of the solar energy, which increases with the increase in the solar radiation.

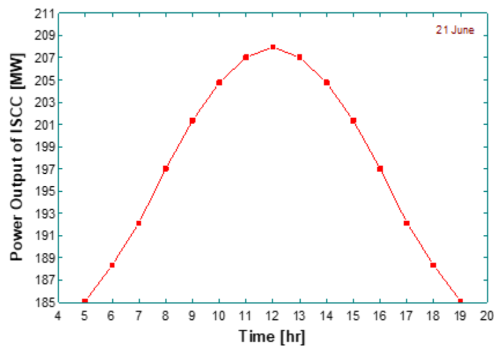

Fig. 9 ISCC power output at selected dates.

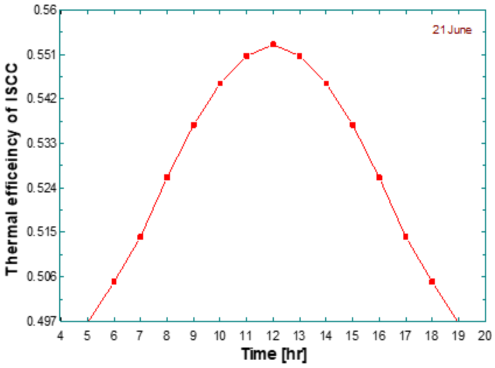

Fig. 10 ISCC efficiency at selected dates.

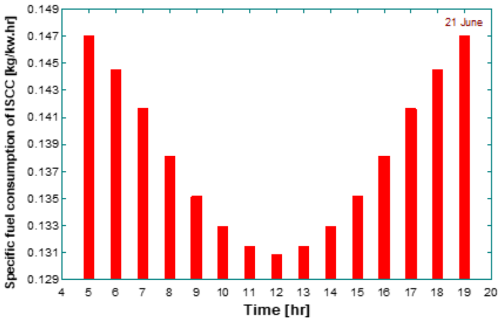

Fig. 11 ISCC specific fuel consumption at selected dates.

4. CONCLUSION

Simulation results show that the ISCC power plant responds positively to solar energy, as the electricity output increases with the increase in solar radiation. The ISCC system's operating mode raises the plant capacity to 207.964 MW and the thermal efficiency to 55.3% at the design point, while the specific fuel consumption decreases to 0.1315 kg/kW.hr. This is due to the increase in the amount of steam produced from the solar energy field, which is added to the HRSG system. The increase in the amount of steam produced from the solar energy field requires an expansion of the solar field area, but this comes at the expense of higher costs to obtain greater power generation capacity and overall efficiency. The system proves to be particularly effective in regions with high solar radiation. Despite the positive results, some limitations need to be considered. The system's performance is highly dependent on solar availability, and its economic feasibility may vary depending on location-specific factors such as land cost, solar intensity, and seasonal fluctuations. Therefore, careful planning and site-specific feasibility studies are essential before implementation. Future research should focus on optimizing the solar field design, improving cost-efficiency, and exploring hybrid solutions that could further enhance system reliability and performance across different climatic conditions.

Table 2: Nomenclature

Symbol	Description
A_{sf}	Solar filed area (m^2)
D_{ro}	Receiver outer diameter (m)
f_{clean}	Cleanliness factor
L	Collector length (m)
LCV	Lower calorific value of the fuel (kJ/kg)
M	Number of collectors (PTC) in each row
$\dot{m}_f$	Mass of exhaust gases leaving the gas turbine unit (kg/s)
Pe_{CCGT}	Power output from combined cycle power plant (MW)
Pe_{sf}	Power generated from the solar filed (MW)
Q_{loss}	Heat losses of collector (kW)
Q_{abs}	solar energy absorbed by collector
w_a	Collector aperture width
ρ_c	Collector reflectance
φ	Latitude angle (Degree)

REFERENCES

[1] B. J. Alqahtani and D. Patiño-Echeverri, "Integrated solar combined cycle power plants : Paving the way for thermal solar," *Applied Energy* ,vol. 169, pp. 927–936, 2016, doi: 10.1016/j.apenergy.2016.02.083.

[2] A. A. Bashir and M. Özbey, "Modelling and analysis of an 80-MW parabolic trough concentrated solar power plant in Sudan," *Clean Energy*, vol. 6, no. 3, pp. 512–527, 2022, doi: 10.1093/ce/zkac032.

[3] Y. Li, J. Yuan, and Y. Yang, "A study on solar multiple for an integrated solar combined cycle system with direct steam generation," *Energy Procedia*, vol. 61, pp. 29–32, 2014, doi: 10.1016/j.egypro.2014.11.898.

[4] J. H. Peterseim, A. Tadros, U. Hellwig, and S. White, "Integrated solar combined cycle plants using solar towers with thermal storage to increase plant performance," *in Proc. ASME 2013 Power Conf.*, vol. 2, V002T08A003, Boston, MA, USA, 2013, doi: 10.1115/POWER2013-98121.

[5] A. Z. Abass and D. A. Pavlyuchenko, "Southern Iraq gas station conversation to integrated solar combined cycle," *E3S Web of Conferences*, vol. 114, Art. no. 05008, 2019, doi: 10.1051/e3sconf/201911405008.

[6] H. M. Benabdellah and A. Ghenaiet, "Energy, exergy, and economic analysis of an integrated solar combined cycle power plant," *Engineering Reports*, vol. 3, no. 11, Art. no. e12404, 2021, doi: 10.1002/eng2.12404.

[7] N. Abed and I. Afgan, "An extensive review of various technologies for enhancing the thermal and optical performances of parabolic trough collectors," *International Journal of Energy Research*, vol. 44, no. 7, pp. 5117–5164, 2020, doi: 10.1002/er.5271.

[8] C. Tzivanidis, E. Bellos, D. Korres, and K. A. Antonopoulos, "Thermal and optical efficiency investigation of a parabolic trough collector," *Case Studies in Thermal Engineering*, vol. 6, pp. 226–237, 2015, doi:10.1016/j.csite.2015.10.005.

[9] M. M. Khan and M. J. Ahmad, "Estimation of global solar radiation using clear sky radiation in Yemen," *Journal of Engineering Science and Technology Review*, vol. 5, no. 2, pp. 12 –19, 2012, doi: 10.25103/JESTR.052.03.

[10] I. T. Toğrul, H. Toğrul and D. Evin, "Estimation of global solar radiation under clear sky radiation in Turkey," *Renewable Energy*, vol. 21, no. 2, pp. 271–287, 2000, doi: 10.1016/S0960-1481(99)00128-7.

[11] C.H. Rossa, J. B. Dias, and G. A. M. Karnas, "Evaluation of energy produced by grid-connected photovoltaic systems in Porto Alegre - Brazil," in *Materials and Processes for Energy: Communicating Current Research and Technological Developments*, A. Méndez-Vilas, Ed., Badajoz, Spain: Formatex Research Center, vol. 1, pp. 45–51, 2013.

[12] Z. M. Thant, M. M. Soe, and M. M. Htay, "Effect of inclination angle on solar radiation of water-in-glass evacuated tubes of domestic water heater," *International Journal of Mechanical and Production Engineering*, vol. 3, no. 6, pp. 15–19, Jun. 2015.

[13] S.A Channiwala and A. Ekbote, "A generalized model to estimate field size for solar-only parabolic trough plant," in Proceedings of the *Third Southern African Solar Energy Conference*, Kruger National Park, South Africa, May 11-13, pp. 283–288, 2015.

[14] A. E. Elmohlawy, B. I. Kazandzhan and V. F. Ochkov, "Modeling and performance prediction of solar parabolic trough collector for hybrid thermal power generation plant under different weather conditions," *in AIP Conference Proceedings*, vol. 2047, no. 020002, 2018, doi: 10.1063/1.5081635.

[15] L. Achour, M. Bouharkat, and O. Behar, "Performance assessment of an integrated solar combined cycle in the southern of Algeria," *Energy Reports*, vol. 4, pp. 207–217, 2018, doi:10.1016/j.egyr.2017.09.003.

[16] E. M. Mokheimer, Y. N. Dabwan, M. A. Habib, S. A. M. Said, and F. A. Al-Sulaiman, "Techno-economic performance analysis of parabolic trough collector in Dhahran, Saudi Arabia," *Energy Conversion and Management*, vol. 86, pp. 622–633, 2014, doi: 10.1016/j.enconman.2014.06.023.

[17] A. E. Elmohlawy, V. F. Ochkov, and B. I. Kazandzhan, "Thermal performance analysis of a concentrated solar power system (CSP) integrated with natural gas combined cycle (NGCC) power plant," *Case Studies in Thermal Engineering*, vol. 14, Art. no. 100458, 2019, doi: 10.1016/j.csite.2019.100458.

[18] A. E. EL-mohlawy, V. F. Ochkov, and B. I. Kazandzhan, "Study and prediction the performance of an Integrated Solar Combined Cycle Power Plant, " *Energy Procedia*, vol. 156, pp. 72–78, 2019, doi: 10.1016/j.egypro.2018.11.094.

تقييم أداء توربينات الغاز ذات الدورة المركبة المتكاملة مع نظام الطاقة الشمسية المركزة

رحمه لقمان ابراهيم
rahma.21enp85@student.uomosul.edu.iq

عبد الرحمن حبو محمد
abidhabbo20@uomosul.edu.iq

قسم الهندسة الميكانيكية, كلية الهندسة, جامعة الموصل, الموصل, العراق

تاريخ الاستلام: 6 مارس 2025 استلم بصيغته المنقحة: 10 يوليو 2025 تاريخ القبول: 3 اغسطس 2025

الملخص

هناك اهتمام كبير بتطوير محطة كهرباء غازية بسيطة، وفي هذا الصدد ناقشنا إمكانية تطوير محطة كهرباء غازية بسيطة بقدرة (125 ميجاوات). وتمثل المرحلة الأولى في الاستفادة من كمية الطاقة الحرارية الخارجة من وحدة التوربين الغازي البسيطة مع غازات العادم عن طريق دمج وحدة التوربين الغازي مع وحدة التوربين البخاري باستخدام مولد بخاري ثنائي الضغط لاستعادة الحرارة، لتكوين الوحدة التوليدية المركبة. أما المرحلة الثانية التي ركزت عليها هذه الدراسة، فتمثلت في الاستفادة من الطاقة الشمسية من خلال دمج الأخيرة مع حقل الطاقة الشمسية، لتكوين الوحدة التوليدية المركبة المتكاملة بالطاقة الشمسية. وتبين النتائج أن التحسن الذي تم الحصول عليه من المرحلة الأولى ان أعلى إنتاج الطاقة وكفاءة الطاقة الحرارية يمكن الحصول عليه وأفضل استهلاك نوعي للوقود هو (185.423 ميجاوات)، (49.77٪) و (0.147 كجم / كيلو وات.ساعة) على التوالي. وفيما يتعلق بالمرحلة الثانية، أظهرت النتائج أن إضافة مجمع شمسي ساهم في زيادة كمية البخار الداخل إلى وحدة البخار ونتيجة لذلك ارتفعت القدرة الناتجة والكفاءة الحرارية لوحدة الدورة المركبة إلى (207.964 ميجاوات) و (55.3٪) ، أما بالنسبة لاستهلاك الوقود النوعي فقد بلغى (0.1315 كجم/كيلو وات.ساعة).

الكلمات الداله :

الوحدة التوربين الغازي ذات الدورة المركبة، الوحدة التوليدية المركبة المتكاملة بالطاقة الشمسية، المجمع الشمسي، مولد بخاري ثنائي الضغط.